AE-456
UDC 621.039.51
539.173.84
621.039.526

AE-456

# Measurement of the Effective Delayed Neutron Fraction in Three Different FRO-cores

L. Moberg and J. Kockum



AKTIEBOLAGET ATOMENERGI

STUDSVIK, NYKÖPING, SWEDEN 1972

ERRATA

to report AE-456

"Measurement of the Effective Delayed Neutron Fraction in Three Different FRO-cores"

L. Moberg and J. Kockum

(Published 1972)

Table 11

| Core | $\frac{\text{No. of fissions in } ^{238}U}{\text{No. of fissions in } ^{235}U}$ | Relative change in $\beta$ for $^{235}U$ | Relative change in $\beta$ for $^{238}U$ |
|---|---|---|---|
| 3 | 0.187 | $2.9 \cdot 10^{-2}$ | $6.8 \cdot 10^{-2}$ |
| 5 | 0.141 | $3.5 \cdot 10^{-2}$ | $10.8 \cdot 10^{-2}$ |
| 8 | 0.155 | $5.2 \cdot 10^{-2}$ | $14.4 \cdot 10^{-2}$ |

AKTIEBOLAGET ATOMENERGI, Sweden 1973

# MEASUREMENT OF THE EFFECTIVE DELAYED NEUTRON FRACTION IN THREE DIFFERENT FR0-CORES

L Moberg and J Kockum


## ABSTRACT

The effective delayed neutron fraction, $\beta_{eff}$, has been measured in the three cores 3, 5 and 8 of the fast zero-power reactor FR0. The variance-to-mean method, in which the statistical fluctuations of the neutron density in the reactor is studied, was used.

A $^{3}$He-gas scintillator was placed in the reflector and used as a neutron detector. It was made more sensitive to fast neutrons by surrounding it with polythene. Its efficiency, expressed as the number of counts per fission in the reactor, was determined using fission chambers with known efficiency placed in the core. The space distribution of the fission rate in the core was determined by foil activation technique.

The experimental results were compared with theoretical $\beta_{eff}$-values calculated with perturbation theory. The difference was about 3 % which is of the same order as the accuracy in the experimental values.


Printed and distributed in June 1972.

LIST OF CONTENTS

## 1. INTRODUCTION

Systematic discrepancies between calculated and measured central reactivity values in fast critical assemblies have been observed [1], [2]. Also for the FR0-reactor such an effect was found and it amounts to about 20 % for $^{235}U$ in some cores. The possible sources for the disagreement are analyzed in [3] where the contribution from the uncertainty in the delayed neutron data is estimated to give a discrepancy of up to 9 %. The analysis is based on the data given by Keepin [6] and shows that it is mainly the lack of experimental information about the delayed neutron spectrum that causes the error. Some authors [4], [5] claim that the uncertainty in the delayed neutron yields is larger than what is given by Keepin, while other experiments [7] confirm the Keepin data.

The uncertainty in the delayed neutron data has motivated an integral measurement of the effective delayed neutron fraction, $\beta_{eff}$, in FR0. Possible methods are discussed in [8] where the variance-to-mean method is considered suitable in small fast assemblies. This method requires a calibration of the detector expressed as the number of counts/fission in the reactor. For this purpose miniature fission chambers [9] used in other FR0 experiments and with known efficiency could be utilized.

Variance-to-mean experiments were performed in three cores: 3, 5 and 8. All the cores contain uranium-fuel with an enrichment of 20 % $^{235}U$. The construction of the reactor is described in [9] and the atom densities in the different cores are given in Appendix 1. Calculated neutron spectra are shown in Fig 1.

## 2. PRINCIPLES OF THE VARIANCE-TO-MEAN EXPERIMENT

A detector with high efficiency is placed in the reactor. The number of detections during short time intervals are recorded while the reactor is run slightly subcritical. The neutrons from spontaneous fission in the fuel will yield a neutron density that fluctuates in a statistical way around a mean value. By determining the variance of the recorded number of counts one will get a measure of these fluctuations. If the detector efficiency is high enough to detect two or more neutrons that have their origin in the same spontaneous fission neutron, i.e. belong to the same fission chain, the variance will be considerably larger than if the counts were independent of each other.

Assuming that the lumped parameter model of the reactor (point reactor model) is valid the variance-to-mean ratio is given by (see for instance [ 10 ]):

$$\frac{\overline{m^2}-\overline{m}^2}{\overline{m}} = 1 + \frac{\epsilon D_\nu}{\rho_p^2}\left(1 - \frac{1-e^{-\alpha\tau}}{\alpha\tau}\right) \qquad (1)$$

where

$m$ = number of counts during time $\tau$

$\epsilon$ = detector efficiency in counts/fission

$D_\nu = \frac{\overline{\nu^2}-\overline{\nu}}{\overline{\nu}^2}$ the dispersion in $\bar{\nu}$

$\nu$ = number of prompt neutrons/fission

$\rho_p = \frac{\rho-\beta_{eff}}{1-\beta_{eff}}$ prompt reactivity

$\rho$ = reactivity

$\alpha = \frac{[\rho]}{\ell}$ the so called Rossi-$\alpha$

$\ell$ = neutron lifetime

Bars denote average values.

For counts independent of each other, i.e. distributed according to the Poisson law, the following is valid:

$$\frac{\overline{m^2}-\overline{m}^2}{\overline{m}} = 1$$

To obtain the maximum information about $\beta_{eff}$ the three parameters $\epsilon$, $\rho$ and $\tau$ should be chosen in a suitable combination. However, to make this optimization we must consider a more complete description of the variance-to-mean ratio given by Bennett [ 11 ]

$$\frac{\overline{m^2}-\overline{m}^2}{\overline{m}} = 1 + 2\,\epsilon D_\nu \sum_{p=1}^{7} \frac{A_p T(s_p)}{s_p}\left(1 - \frac{1-e^{-s_p\tau}}{s_p\tau}\right) \qquad (2)$$

where T(s) is the transfer function of the reactor and could be expressed as

$$T(s) = \sum_{p=1}^{7} \frac{A_p}{s+s_p}$$

In the derivation of Eq (2) the point reactor model is also assumed but the effect of the delayed neutrons is taken into account while they were omitted in Eq (1). Therefore, by omitting all the terms for $p > 1$ in Eq (2) we will again arrive at Eq (1).

Eq (2) can be rewritten as

$$\frac{\overline{m^2}-\overline{m}^2}{\overline{m}} = 1 + \varepsilon D_\nu \cdot \left[\frac{1-\beta_{eff}}{\beta_{eff}-\rho}\right]^2 \left(1 - \frac{1-e^{-\alpha\tau}}{\alpha\tau}\right) +$$

$$+ 2\,\varepsilon D_\nu \sum_{p=2}^{7} \frac{A_p T(s_p)}{s_p} \left(1 - \frac{1-e^{-s_p\tau}}{s_p}\right) \qquad (3)$$

The information about $\beta_{eff}$ lies in the second term on the right hand side of Eq (3) and obviously this term should be made as large as possible in comparison to the other two.

The second term is made large by choosing

i) $\varepsilon$ as large as possible
ii) $|\rho|$ small in comparison to $\beta_{eff}$
iii) $\tau$ big enough to make the value of the expression

$1 - \frac{1-e^{-\alpha\tau}}{\alpha\tau}$ near equal to 1.

However, the last term in Eq (3) is also dependent on these parameters. It was calculated starting from the transfer-function with the parameters given in [12] and with a theoretical value of $\beta_{eff}$. When this term is kept small it could be taken into account by a correction factor on the second term. The correction for different values of $\rho$ and $\tau$ are shown in Fig 2.

Typical values of the parameters in an experiment are $\tau = 5 \cdot 10^{-3}$ s; $-\rho = 3 \cdot 10^{-4}$; $\epsilon = 3 \cdot 10^{-4}$

which give $\frac{\overline{m^2} - \overline{m}^2}{\overline{m}} \approx 5$.

The variance-to-mean expression has been derived in [12] assuming a tworegion reactor model instead of the point reactor model. This gives a similar expression with the $\beta_{eff}$-dependence included in one term and with higher-order correction terms. These were calculated and no significant difference from the point reactor case was found. Thus, the point reactor model could be accepted.

## 3. DESCRIPTION OF THE EXPERIMENT

### 3.1 The detector

The detector was designed to fulfil the following requirements:

a) high efficiency for fast neutrons
b) short dead-time
c) effective discrimination between neutron- and $\gamma$-detections.

The conditions b) and c) could be met by a gas-scintillator containing $^3$He+Xe-gas. To satisfy condition a) the detector was surrounded by a layer of polythene.

The scintillator consisted of a one inch diameter, two inch high cylindrical Kovar vessel with a plane glass window. The walls were internally coated with MgO for light reflection and furnished with a thin layer of quaterphenyl acting as a wave length shifter. The vessel was filled with a mixture of 80 % $^3$He and 20 % Xe to a total pressure of 3 atm. It was coupled to a small photomultiplier (EMI 9524 E).

The pulse-height distribution of the photomultiplier pulses after amplification is shown in Fig 3. Here a $^{242}$Cm-Be-source was used which gives high energy neutrons and relatively little $\gamma$-radiation. The corresponding pulse-height distribution for neutrons from the reactor is quite similar.

A sketch of the detector with the surrounding polythene is shown in Fig 4 and its position in the reflector of the reactor can be seen in Fig 5. Between the polythene and the copper a 0.5 mm thick layer of cadmium is inserted.

The time delay of the neutrons in the polythene before detection and its effect on the variance-to-mean expression has been investigated and is described in [13]. It was found that the variance-to-mean expression is very little affected except for the dead time corrections which are changed by about a factor of 2. This is further discussed in Section 8 in connection with the dead time corrections.

### 3.2 Electronics and data collection equipment

A block diagram of the electronics is shown in Fig 6.

The signal from the photomultiplier is amplified, double-delay clipped with a clipping time of 250 ns and passes a fast discriminator before going to a scaler. With a control unit the scaler is made to record the number of counts during the time $\tau$. This number is registered on a paper tape and the scaler starts counting again. The procedure is repeated with a frequency which is limited by the printing time and is about 4 cycles per second.

A complete experimental run includes $10^4$ cycles which takes about 45 minutes.

## 4. DETERMINATION OF THE VARIANCE-TO-MEAN RATIO

### 4.1 Method

The ratio between the variance ($s^2$) and the mean value ($\bar{m}$) of the registered numbers was calculated in the following way:

The data were divided into subgroups of 200 consecutive registrations each. In each group $s^2$ and $\bar{m}$ was calculated and the mean value of $s^2/\bar{m}$ from all the groups was determined.

The reason for the division of the data into subgroups was the unavoidable slow fluctuations in reactor power. However, the effect was small: the difference between $s^2/\bar{m}$ taken from the data as a whole and from a mean value between the subgroups was about 1 %.

The data were carefully examined to eliminate false registrations. Those subgroups were omitted which had an unexpectedly high variance or a probability distribution of m, which in the sense of the $\chi^2$-test deviated too much from the distribution of all the data. Only a few subgroups were discarded during the whole experiment.

## 4.2 Standard deviation of the variance-to-mean ratio

The standard deviation of $s^2/\bar{m}$ is given in [14] as

$$\frac{\delta(s^2/\bar{m})}{s^2/\bar{m}} = N^{-1/2} \left[ 2 + \frac{1}{\bar{m}} \cdot \frac{s^2}{\bar{m}} \right]^{1/2} \qquad (4)$$

where N is the total number of registrations.

Obviously the method of dividing the data into subgroups yields the same standard deviation as treating all the data in one group.

The variance between the $s^2/\bar{m}$-values in the subgroups was also studied and gave an observed standard deviation of the mean that was slightly larger than the one given in Eq (4).

Typical values are for $N = 10^4$:

observed relative standard deviation: $2.2 \cdot 10^{-2}$
relative standard deviation from Eq (4): $1.6 \cdot 10^{-2}$.

The difference could be explained by the slow fluctuations in power level during a measurement. In the error analysis the observed standard deviation was used.

## 4.3 Correlation between consecutive registrations

When the experiment is performed under suitable conditions, there should be a correlation between the counts during the counting interval $\tau$, but negligible correlation between the counts in successive counting intervals. A theoretical investigation of these effects is given in [14] and was considered when the values of $\tau$ and the time between the counting intervals were chosen for our experiment.

A check of the experimental data was made by calculating the values of the correlational functions which describe the correlation between the number of counts in successive intervals. The result was compared with the theoretical values from [14] and within the statistical accuracy no disagreements were found.

## 4.4 Check with a Poisson distributed source

As mentioned in Section 2 the variance-to-mean ratio for Poisson distributed counts equals unity.

By using a $^{242}$Cm-Be-source the electronic equipment was checked and the result of a series of measurements is given in Table 1.

Table 1

| | $s^2/\bar{m}$ |
|---|---|
| | 1.008 ± 0.014 |
| | 0.984 ± 0.014 |
| | 0.990 ± 0.014 |
| | 1.010 ± 0.014 |
| mean value | 0.998 ± 0.007 |

In each of these measurements the number of registrations was $10^4$.

## 5. EFFICIENCY CALIBRATION OF THE DETECTOR

### 5.1 Method

The efficiency of the $^3$He-scintillator should be determined expressed as the number of counts per fission in the reactor.

First the relation between the number of counts in the scintillator and the fission rate in the centre of the core was determined. During a variance measurement the scintillator was calibrated relative to a $^3$He-proportional counter which was very stable. Before or after the experiment the central fuel element was changed to a fuel element containing a miniature fission chamber with known efficiency. The proportional counter and the fission chamber were calibrated relative to each other. Since the difference in the efficiency of the detectors was rather large the calibration was divided into two intermediate steps using two other fission chambers placed in the reflector. The position of all the detectors is shown in Fig 5.

The relation between the central and the mean fission rate in the core had also to be determined. The fission rate distribution over the core was measured with foil activation technique. A two dimensional function was fitted to the measured points and integrated over the core volume. The mean value of the fission rate in the core was obtained by dividing with the volume.

An analytic expression for the detector efficiency is given in Appendix 2 and shows which properties had to be measured.

## 5.2 Fission rate measurements

The fission chambers used in the centre of the core are described in [15]. One of them contained natural uranium and the other enriched uranium (93 % $^{235}U$). They had been calibrated in the sense that the relation between the count rate and the fission rate in $^{235}U$ and $^{238}U$ had been determined.

The spatial distribution of the fission rate, $R_{25}(r,z)$ and $R_{28}(r,z)$, was measured with foil activation technique. For measuring $R_{25}(r,z)$ U-Al-foils with ~ 90 % enriched $^{235}U$ were used. The foils were calibrated by measuring the natural $\gamma$-activity at 185 keV. For $R_{28}(r,z)$ U-metal-foils either in natural form or depleted to 0.4 % $^{235}U$ were used. The intercalibration among these was done by weighing. After activation the $\gamma$-activity from the fission products was measured. The lower level of the measured $\gamma$-activity was chosen as 400 keV for the $^{235}U$-foils and 600 keV for the $^{238}U$-foils.

The foils were placed in 25 positions in the core: in 5 different axial positions in all the 5 fuel elements on a radius. The position within a fuel element is shown in Fig 7. Earlier investigations have shown that the distribution is symmetric around the centre and the axis of the cylindrical core, so that the distribution in the whole core can be obtained from this measurement.

A typical space distribution can be seen in Fig 8. The $\gamma$-activity was measured with a statistical accuracy of 0.3 - 0.6 %. In order to check that there were no other big sources of error the data were divided into several groups and the variance of the result was studied.

A small correction for the content of $^{235}U$ in the $^{238}U$-foils had to be made, because the fission rate distribution was a little different for the two isotopes. This correction amounts to about 3 % near the core edge.

## 5.3 Integration of the fission rate distribution

A two-dimensional function in cylinder geometry was fitted to the experimental points describing the space distribution of the fission rate.

In order to smooth the statistical fluctuations a slowly varying function should be used. However, it should still be of high enough order to fit the true distribution.

A computer code [16] that fits a rational function by the least squares method was used. Various degrees of the polynomials in the numerator and the denominator were tried and it was found that a good enough fit was achieved by a polynominal function (constant denominator) of the form

$$R(r,z) = c_o + c_1 r^2 + c_2 z^2 + c_3 r^2 z^2 + c_4 r^4 + c_5 z^4 + c_6 r^2 z^4 +$$

$$+ c_7 r^4 z^2 + c_8 r^4 z^4$$

In order to integrate this function in cylinder-geometry the irregular core edge must be approximated by a smooth cylinder surface. A computer program [17] was used which calculates an equivalent radius $r_e$ from the relation

$$\iint_A \Phi(r)dxdy = \int_o^{r_e} \Phi(r)dr$$

where the integration on the left hand side is made over the core area, A, for z = 0. By using $\Phi(r) = R(r,o)$, $r_e$ will denote the radius for a cylinder which gives the same mean fission rate as the irregular core.

The integration of R(r,z) over the core volume was made numerically and yielded the factors $k_{25}$ and $k_{28}$, defined in Appendix 2.

## 5.4 Correction for the spectrum dependence of the fission product γ-radiation yield

The yield of the γ-activity above a certain energy level is slightly dependent on the energy of the neutron causing the fission. As the neutron spectrum in the core changes close to the copper-reflector a correction has to be made to the measured fission rate distribution. This correction was based on an investigation for core 3 described in [18] and is defined as a correction factor for $k_{25}$ and $k_{28}$.

The following correction factors were used for $^{235}U$

| Core | Correction |
|---|---|
| 3 | $1.013 \pm 0.007$ |
| 5 | $1.007 \pm 0.007$ |
| 8 | $1.010 \pm 0.007$ |

The values for cores 5 and 8 are estimated from the value of core 3. For $^{238}U$ the correction is negligible.

## 5.5 Heterogeneity effects

The absolute value of the fission rate in the centre of the core was measured with the fission chambers in a hole in a homogenized zone of the central fuel element, which is shown in Fig 9. Compare with Fig 7 which shows the foils placed in a normally loaded fuel element. This way of placing the foils will be called "normal".

A better way to measure the mean fission rate within a module is to place the foils within the uranium plates (see Fig 9). This will be denoted "heterogeneous" placing.

The following relations were investigated:

i) The ratio, $K_i$, between the fission rate with "heterogeneous" placing of foils in the centre of the core and with a foil near the fission chamber in the homogenized zone.

$$K_i = \left( \frac{R_{Heterog.}}{R_{Homog.}} \right)_{centre}$$

$K_i$ relates the fission rate measured by fission chamber and the true fission rate in the centre. $k_{25}$ and $k_{28}$ were multiplied by $K_i$ for the corresponding isotope.

ii) The ratio $K_{ii}$ which describes the difference between the "heterogeneous" and "normal" way to place the foils at the core edge and at the centre, respectively.

$$K_{ii} = \left( \frac{R_{Heterog.}}{R_{normal}} \right)_{edge} \Big/ \left( \frac{R_{Heterog.}}{R_{normal}} \right)_{centre}$$

$K_{ii}$ describes the difference in the fission rate distribution measured in the "normal" way and in the "heterogeneous" way.

The results obtained are given in Table 2.

Table 2

| Core | Isotope | $K_i$ | $K_{ii}$ |
|---|---|---|---|
| 3 | $^{235}U$ | 1.003 ± 0.006 | 0.993 ± 0.009 |
| 3 | $^{238}U$ | 1.052 ± 0.010 | 0.993 ± 0.014 |
| 5 | $^{235}U$ | 1.001 ± 0.008 | — |
| 5 | $^{238}U$ | 1.008 ± 0.009 | — |
| 8 | $^{235}U$ | 0.980 ± 0.007 | 0.991 ± 0.010 |
| 8 | $^{238}U$ | 0.998 ± 0.007 | 0.991 ± 0.012 |

$K_{ii}$ differs very little from 1 and its influence is neglected.

Another effect that could also be neglected was the influence from the central hole on the fission rate distribution outside the core.

### 5.6 Results of the calibration

The values of $k_{25}$ and $k_{28}$ after corrections and one example of the efficiency $\varepsilon$ for one experimental run on each core are given in Table 3.

Table 3

| Core | $k_{25}$ | $k_{28}$ | $\varepsilon \cdot 10^4$ counts/fission |
|---|---|---|---|
| 3 | 0.657 ± 0.010 | 0.579 ± 0.008 | 4.07 ± 0.09 |
| 5 | 0.648 ± 0.010 | 0.606 ± 0.011 | 3.29 ± 0.07 |
| 8 | 0.638 ± 0.009 | 0.568 ± 0.013 | 3.25 ± 0.07 |

## 6. DISPERSION IN $\bar{\nu}$

The factor $D_\nu = \frac{\overline{\nu^2} - \bar{\nu}}{\bar{\nu}^2}$ for the case of $^{235}U$ was calculated from the experimental data from an integral measurement of $\bar{\nu}$ in the different cores of FR0 [19]. For $^{238}U$ the factor was known only for discrete

neutron energies [20] and it was averaged over a theoretical reactor spectrum. $D_\nu$ for the two isotopes were weighted in accordance with the total number of fissions in each isotope and a mean value was calculated.

The values given in Table 4 were used.

Table 4

| Core | $D_\nu(^{235}U)$ | $D_\nu(^{238}U)$ | $D_\nu$(mean) |
|---|---|---|---|
| 3 | 0.800 ± 0.011 | 0.827 ± 0.025 | 0.804 ± 0.015 |
| 5 | 0.813 ± 0.020 | 0.827 ± 0.025 | 0.815 ± 0.021 |
| 8 | 0.803 ± 0.012 | 0.827 ± 0.025 | 0.806 ± 0.015 |

For thermal neutron induced fission in $^{235}U$ the value of $D_\nu$ is 0.798 as given in [21].

## 7. DETERMINATION OF THE SUBCRITICALITY

The factor in Eq (1) which contains the desired information about $\beta_{eff}$ is

$$\rho_p = \frac{\rho - \beta_{eff}}{1 - \beta_{eff}}$$

where the reactivity $\rho$ was determined by the positive period technique in the following way:

A control rod (fuel loaded) was fully inserted when the reactor was stable on the subcriticality level used in the experiment. The exponential increase in power was monitored. Then, using another control rod the reactor was stabilized at a high power level where it could be considered as critical. The first control rod was inserted again in exactly the same way as in the first run and the power increase was monotored. The supercriticality in these two situations was calculated from the "in-hour"-equation and the difference yielded the subcriticality level used in the variance measurement.

The "in-hour"-equation, which gives the value $\rho$, contains the parameters $\beta_{k,eff}$, the effective delayed neutron fraction in group k. The assumption of six delayed neutron groups is made and $\beta_{eff}$ is given by

$$\beta_{eff} = \sum_{k=1}^{6} \beta_{k,eff}$$

Now, if $|\rho|$ is limited to a small value in comparison with $\beta_{eff}$ an iteration procedure can be used: An expected value of $\beta_{eff}$ if first used to evaluate $\rho$ which then gives a better $\beta_{eff}$-value and so on. In practice only two iteration steps were needed as long as $|\rho|$ was limited to a value of less than about 15 % of $\beta_{eff}$. In this case we can also tolerate a rather large error in $\rho$ without considerable influence on $\beta_{eff}$.

A lower limit of $-\rho$ was given in Section 2 to about 10 pcm.

Examples of the iteration steps for experimental runs with different values of $-\rho$ are given in Table 5 (all values in pcm).

Table 5

| Core | $\beta_{eff}^{(o)}$ | $-\rho^{(1)}$ | $\beta_{eff}^{(1)}$ | $-\rho^{(2)}$ | $\beta_{eff}^{(2)}$ | $-\rho^{(3)}$ | $\beta_{eff}^{(3)}$ |
|---|---|---|---|---|---|---|---|
| 3 | 703.4 | 94.5 ± 3.0 | 712.5 | 96.8 | 710.2 | 96.5 | 710.5 |
| 3 | 703.4 | 56.6 ± 3.0 | 723.6 | 58.0 | 722.2 | 57.9 | 722.3 |
| 5 | 715.2 | 38.5 ± 3.0 | 750.2 | 40.1 | 749.5 | 40.1 | 749.5 |
| 8 | 706.4 | 26.3 ± 3.0 | 731.2 | 27.1 | 729.6 | 27.0 | 729.7 |

$\beta_{eff}^{(o)}$ are the theoretical values (see Section 10).

## 8. DEAD-TIME CORRECTION

The dead-time of the equipment was determined by calibrating the $^3$He-scintillator at different power levels against another detector with a lower count rate. It was expected that the dead-time should be defined by the pulse clipping time to 250 ns, buth it was found to be larger and also to be dependent on the setting of the discriminator level. This could be explained by a saturation effect in the photomultiplier which lowered the pulse height at high count rates.

The dead-time was determined as 1.5 and 3.4 μs for the discriminator levels used.

The dead-times measured in this way were checked by making a variance-to-mean experiment on a Poisson-distributed source for

rather high count rates. When the dead-time correction had been applied (see below) the result was equal to 1 within the limits of the statistical errors.

The dead-time corrections in the variance-to-mean expression are given in [ 13] where also the effect of the time delay of neutrons in the polythene surrounding the detector is taken into account.

$$\frac{\overline{m_d^2}-\overline{m_d}^2}{\overline{m_d}} = 1 - A(d) + \frac{\varepsilon_d D_\nu}{\rho_p^2} \cdot \frac{\tau-d}{\tau} \cdot B(d) \cdot \left[ 1 - \frac{\alpha_r^2}{\alpha_r^2-\alpha_d^2} \cdot \frac{B_d \cdot e^{-\alpha_d d}}{B(d)} \cdot \right.$$

$$\left. \cdot \frac{1-e^{-\alpha_d(\tau-d)}}{\alpha_d(\tau-d)} - \frac{\alpha_d^2}{\alpha_d^2-\alpha_r^2} \cdot \frac{B_r \cdot e^{-\alpha_r d}}{B(d)} \cdot \frac{1-e^{-\alpha_r(\tau-d)}}{\alpha_r(\tau-d)} \right]$$

with

$$A(d) = \overline{m_d} \left[ 1 - \left(\frac{\tau-d}{d}\right)^2 \right]$$

$$B(d) = \frac{\alpha_r^2 \cdot B_d \cdot e^{-\alpha_d d} - \alpha_d^2 B_r \cdot e^{-\alpha_r d}}{\alpha_r^2-\alpha_d^2}$$

where

$m_d$ = number of counts during time $\tau$

$\varepsilon_d$ = detector efficiency in the presence of a dead-time d

$\alpha_r$ = the Rossi-$\alpha$ for the reactor ($\alpha_r = 5.0 \cdot 10^4$ for core 3)

$\alpha_d$ = a constant describing the delay in the polythene given in [ 13] as $\alpha_d = 2.8 \cdot 10^4\ s^{-1}$

$B_r$, $B_d$ are rather complicated functions of the variables given above and can be found in [ 13].

An example of the values of the correction terms for two different experimental runs are given in Table 6.

Table 6

| d μs | A(d) | $\frac{\tau-d}{\tau}$ | $B_r$ | $B_d$ | B(d) | Total dead-time correction factor in the value of $\beta_{eff}$ |
|---|---|---|---|---|---|---|
| 1.5 | 0.006 | 1.000 | 0.980 | 0.986 | 0.964 | $0.982 \pm 0.008$ |
| 3.4 | 0.010 | 0.999 | 1.003 | 0.994 | 0.939 | $0.969 \pm 0.015$ |

## 9. EXPERIMENTAL RESULTS AND DISCUSSION OF ERRORS

The results of the measurements are given in detail in Appendix 2 and are summarized in Table 7.

Table 7

| Core | $\beta_{eff} \cdot 10^3$ | Error (%) | |
|---|---|---|---|
| | | Type I | Type II |
| 3 | 7.19 | 0.7 | 2.1 |
| 5 | 7.35 | 1.0 | 2.2 |
| 8 | 7.35 | 0.9 | 2.0 |

A distinction between two types of errors is made: Type I which describes the statistical uncertainty in the determination of the variance-to-mean ratio and type II which includes the uncertainty in all the other factors ($\varepsilon$, $D_\nu$, o and the correction factors). The type I-error is only dependent on the number of registrations that are made and could obviously be made infinitely small. The error of type II on the contrary is dominated by some factors in the calibration procedure, in the determination of the factor $D_\nu$ etc which could not be improved and which are determined only once for each core. All summing of the errors are made in quadrature.

The contribution from each of the involved parameters will now be discussed in detail:

The variance-to-mean ratio $\frac{\overline{m^2}-\overline{m}^2}{\overline{m}}$ is considered to have only a random error which is given by the estimated standard error of the mean of the data divided into about 50 subgroups. The standard error is 2.0 - 2.4 % in one experimental run.

Detector efficiency $\varepsilon$: The foil activation was done with a statistical accuracy of 0.3 - 0.6 %. The error in the integration procedure was estimated to be 0.6 % from the uncertainty in the fit and 0.5 % from the approximation of a cylindrical core edge and the uncertainty in the measured fission rate near the edge. The heterogeneity effect is measured with a statistical accuracy of 0.8 % and the quoted error in the yield correction is 0.7 %. The efficiency of the absolutely calibrated fission chambers is known with 1.6 % accuracy and the calibration of these against the $^{3}$He-proportional counter that was used as a monitor during the experiment was made with a statistical accuracy of 1.0 %. The stability of the $^{3}$He-proportional counter was investigated and no drift was found. Finally, the error in the total number of fissile isotopes in the reactor is estimated to 0.5 %.

By using Eq (8) and adding the errors in quadrature one gets a total error in $\varepsilon$ of 2.2 %.

The $D_{\nu}$-factor for $^{235}$U was calculated from the primary data for $\bar{\nu}$ measurements in core 3. The available data were divided into 8 groups and this yielded an estimated standard error of 1.4 %. By comparing the total amount of data available for the three cores 3, 5 and 8 the errors in cores 5, 8 were estimated. However, in core 5 a higher background made the evaluation a little more inaccurate so the error was estimated to be somewhat larger. The error in $^{238}$U was given in [ 12 ] to be 3 %. The weighting of the values for the two isotopes together yielded a final error in $D_{\nu}$ of 1.8 % for cores 3 and 8 and 2.6 % for core 5.

In the subcritical measurement the reactivity difference between two stable power levels was measured by adding the same amount of reactivity to the reactor by inserting a control rod and measuring the exponential increase. The involved sources of errors (statistical uncertainty in the counting, temperature variation, reproducibility in control rod settings, deviation from criticality of the upper power level) were all estimated to give less than 1 pcm error each. The upper limit of the total error was estimated to 3 pcm and this gave an error in $\beta_{eff}$ of 0.4 %. No extra error was assumed to be introduced by the iteration process in which the $\beta_{eff}$- and the $\rho$-value were changed.

Unfortunately the dead-time corrections introduced an uncertainty which could have been avoided by a properly working electronic system with a shorter dead-time. Even if the determination of the dead-time is rather accurate the formulae for the correction are based on an approximation, and an upper limit of the final error was estimated to be 50 % of the correction. This error will contribute to the total error in $\beta_{eff}$ with a max of 1.5 %. The only important term in the correction is B(d), which contains the factors $B_r$ and $B_d$. These are calculated starting from the determined values of $s^2/\bar{m}$ which include an error of type I. However, B(d) is much more strongly affected by the values of $\alpha_r$, $\alpha_d$ and d and is hence considered to be of type II.

The correction due to delayed neutrons (the third term in the variance-to-mean expression Eq (3)) is small and is not considered to introduce any significant error.

## 10. THEORETICAL CALCULATION OF $\beta_{eff}$

Theoretical calculations of $\beta_{eff}$ were made with perturbation theory. The following expression was used

$$\beta_{k,eff} = \frac{\int dV \sum_{i=1}^{N} (\beta_{25,k}\,\bar{\nu}_{25} \cdot \Sigma^i_{25,f} + \beta_{28,k} \cdot \bar{\nu}_{28} \cdot \Sigma^i_{28,f})\phi_i \sum_{j=1}^{N} \chi_j^{k,D}\,\phi_j^+}{\int dV \sum_{i=1}^{N} (\bar{\nu}_{25}\Sigma^i_{25,f} + \bar{\nu}_{28}\Sigma^i_{28,f})\phi_i \sum_{j=1}^{N} \chi_j \phi_j^+}$$

$$\beta_{eff} = \sum_{k=1}^{6} \beta_{k,eff}$$

where

| | | |
|---|---|---|
| N | = | number of energy groups |
| $\phi_i$, $\phi_i^+$ | = | flux and adjoint flux in energy group i ($n \cdot cm^{-2} \cdot \cdot sec^{-1}$) |
| $\chi_j$ | = | fission source in energy group j |
| $\chi_j^{k,D}$ | = | delayed neutron fission source in energy group j for delayed neutron group k |
| $\beta_{25,k}$, $\beta_{28,k}$ | = | delayed neutron fraction for group k in $^{235}U$ and $^{238}U$, respectively |
| $\bar{\nu}_{25}$, $\bar{\nu}_{28}$ | = | average number of prompt fission neutrons in $^{235}U$ and $^{238}U$, respectively |
| $\Sigma^i_{25,f}$, $\Sigma^i_{28,f}$ | = | macroscopic fission cross section in energy group i for $^{235}U$ and $^{238}U$, respectively |

$\phi_i$ and $\phi_i^+$ were calculated in spherical geometry with the code DTF IV with 25 energy groups in the ABN-structure.

The delayed neutron data $\beta_\ell$ and $\chi_j^D$ were taken from Keepin [6]. The delayed neutron spectra $\chi_j^{D^\ell}$ given in this reference originate from a measurement by Batchelor and Hyder [22] and include only the first 4 delayed neutron groups. For groups 5 and 6 the same spectrum as for group 4 was used. The result is given in Table 8.

Table 8: Calculated $\beta_{eff}$-values

| Delayed neutron group k | Input data $\beta_{k,\ell}$ | | $\beta_{k,eff} \cdot 10^3$ | | |
|---|---|---|---|---|---|
| | $^{235}U$ | $^{238}U$ | core 3 | core 5 | core 8 |
| 1 | 0.24 | 0.19 | 0.214 | 0.225 | 0.219 |
| 2 | 1.36 | 2.03 | 1.332 | 1.371 | 1.345 |
| 3 | 1.20 | 2.40 | 1.266 | 1.297 | 1.276 |
| 4 | 2.60 | 5.74 | 2.828 | 2.875 | 2.840 |
| 5 | 0.82 | 3.33 | 1.106 | 1.102 | 1.100 |
| 6 | 0.17 | 1.11 | 0.288 | 0.282 | 0.284 |

The importance of a detailed energy spectrum for the calculation was checked by performing the same calculation with only one energy group (mean energy) in the delayed neutron spectrum. As seen in Table 9 the difference is small.

Table 9

| $\beta_{eff} \cdot 10^3$ | | |
|---|---|---|
| Core | With delayed neutron spectrum from [22] | With one energy group spectrum |
| 3 | 7.034 | 7.044 |
| 5 | 7.152 | 7.144 |
| 8 | 7.064 | 7.065 |

## 11. CONCLUSIONS

The experimental and calculated $\beta_{eff}$ values are compared in Table 10.

Table 10

| | $\beta_{eff} \cdot 10^3$ | | | |
|---|---|---|---|---|
| Core | Exp | Error (%) | Calc | Calc/Exp |
| 3 | 7.19 | 2.2 | 7.03 | 0.978 |
| 5 | 7.35 | 2.4 | 7.15 | 0.973 |
| 8 | 7.35 | 2.2 | 7.06 | 0.961 |

The calculated $\beta_{eff}$ value is directly proportional to the delayed neutron fraction $\beta$, where the values (given by Keepin [6]) for the two fissile isotopes are weighted in relation to the total number of fissions in each isotope. It is obvious that these weighting factors (see Table 11) differ by too little between the three cores to make it possible to draw any definite conclusions about to what extent each isotope contributes to the disagreement. However, it is of interest to change the $\beta$-factor for only one isotope at a time in order to get agreement between experimental and calculated $\beta_{eff}$-values. The result of this investigation is given in Table 11 and indicates that somewhat higher values of $\beta$ should be used to fit the calculated $\beta_{eff}$-values to the experimental results.

Table 11

| Core | $\frac{\text{No of fissions in } ^{238}U}{\text{No of fissions in } ^{235}U}$ | Relative change in $\beta$ for $^{235}U$ | Relative change in $\beta$ for $^{238}U$ |
|---|---|---|---|
| 3 | 0.187 | $2.2 \cdot 10^{-2}$ | $14.0 \cdot 10^{-2}$ |
| 5 | 0.141 | $3.2 \cdot 10^{-2}$ | $21.8 \cdot 10^{-2}$ |
| 8 | 0.155 | $4.5 \cdot 10^{-2}$ | $29.1 \cdot 10^{-2}$ |

## 12. ACKNOWLEDGEMENTS

The authors wish to express their gratitude to S Sjöquist for constructing the electronics, to L-E Persson for preparing the gas-scintillator, to R Håkansson for making the theoretical calculations, to K Pörn for making the computer code to evaluate the measurement, to T L Andersson for advising in planning the foil activations and to L Widén for supporting with data about the dispersion in $\bar{\nu}$. B Karmhag, E Nerentorp and A Pettersson also helpfully assisted with the operation of the reactor.

## 13. REFERENCES


1. LITTLE, W. W. Jr., and HARDIE, R. W.,
Discrepancy between measured and calculated reactivity coefficients in dilute plutonium fueled fast criticals
Nucl. Sci. Eng. 36 (1969) p. 115.

2. YOUNG, W. R., and BENNET, R. A.,
FTR critical experiments analysis
Trans. Am. Nucl. Soc. 12 (1969) p. 183.

3. SAPHIER, D., and YIFTAH, S.,
The effect of errors in the delayed-neutron data on fast reactor static and dynamic calculations
Nucl. Sci. Eng. 42 (1970) p. 272.

4. MASTERS, C. F., THORPE, M. M., and SMITH, D. B.,
Measurement of absolute delayed-neutron yields from 14 MeV fission
Trans. Am. Nucl. Soc. 11 (1968) p. 179.

5. KRICK, M. S., and EVANS, A. E.,
Delayed-neutron yield vs energy measurements
Trans. Am. Nucl. Soc. 13 (1970) p. 746.

6. KEEPIN, G. R.,
Physics of nuclear kinetics
Addison-Wesley Publishing Co., Inc., Reading, Massachusetts 1965.

7. CONANT, J. F., and PALMEDO, P. F.,
Measurement of the delayed-neutron fractions for thermal fission of $^{235}U$, $^{239}Pu$ and $^{233}U$
Nucl. Sci. Eng. 44 (1971) p. 173.

8. BOHN, E. M., KARAM, R. A., and LONG, A. B.,
An evaluation of methods to measure the effective delayed-neutron fraction
Reactor Physics Division Annual Report, July 1, 1968 - June 30, 1969. 1970
(ANL-7610) p. 384.

9. ANDERSSON, T. L.,
Experimental and theoretical work at the zero-energy fast reactor FR0
Proceedings of the international conference on fast critical experiments and their analysis. October 10 - 13, 1966. [1967]
(ANL-7320) p. 159.

10. UHRIG, R. E.,
Random noise techniques in nuclear reactor systems
The Ronalds Press Company, New York 1970, p. 60.

11. BENNETT, E. F.,
The Rice formulation of pile noise
Nucl. Sci. Eng. 8 (1960) p. 53.

12. BERGSTRÖM, A. et al.,
Pulsed source, Rossi-α and variance-to-mean measurements performed at the FR0 reactor
Proc. of the intern. conf. on fast critical experiments and their analysis. October 10 - 13, 1966. [1967]
(ANL-7320) p. 694.

13. MOBERG, L.,
AB Atomenergi, Sweden. 1972.
(Internal report RF-72-301.)

14. PAL, L.,
Determination of the prompt neutron period from the fluctuations of the number of neutrons in a reactor
Reactor Science and Technology (Journal of Nuclear Energy Parts A/B)
17 (1963) p. 395.

15. ANDERSSON, T. L.,
AB Atomenergi. 1964.
(Internal report FFX-1.)

16. TOLLANDER, B.,
AB Atomenergi, Sweden. 1971.
(Internal report RD-28.)

17. TIRÉN, L. I., and AHLIN, Å.,
AB Atomenergi, Sweden. 1964.
(Internal report TPM-RFN-159; TPM-RFX-331.)

18. WENNERBERG, D.,
AB Atomenergi, Sweden. 1971.
(Internal report TPM-RF-71-252.)

19. CONDÉ, H., and WIDÉN, L.,
Private communication

20. CONDÉ, H., and HOLMBERG, M.,
Private communication

21. BOLDEMAN, J. W., and DALTON, A. W.,
Prompt nubar measurements for thermal neutron fission. 1967
(AAEC/E172)

22. BATCHELOR, R., and HYDER, H. R. McK.,
The energy of delayed neutrons from fission
J. Nucl. Energy 3 (1956) p. 7.

## APPENDIX 1

Atomic densities and geometrical dimensions in FR0 cores 3, 5 and 8 ($10^{22}$ atoms/$cm^3$)

| Core | $^{235}U$ [1] | $^{238}U$ | C | H | Fe | Cr | Ni | Al | Cu | Core height cm | Equivalent core radius [2] cm | Refl thickness | |
|---|---|---|---|---|---|---|---|---|---|---|---|---|---|
| | | | | | | | | | | | | axial cm | radial cm |
| 3 | 0.568 | 2.234 | 2.47 | — | 0.408 | 0.096 | 0.048 | — | — | 38.7 | 20.4 | 36.6 | 31 |
| 5 | 0.498 | 1.963 | 2.77 | 0.604 | 0.408 | 0.096 | 0.048 | — | — | 38.7 | 17.9 | 36.6 | 32 |
| 8 | 0.498 | 1.963 | 2.55 | 0.151 | 0.408 | 0.096 | 0.048 | 0.34 | — | 38.7 | 21.9 | 36.6 | 30 |
| Cu-reflector | — | — | — | — | 0.408 | 0.096 | 0.048 | — | 7.48 | — | — | — | — |

1) Including 0.16 % $^{234}U$

2) Valid for heterogeneous core

# APPENDIX 2

The relationship between the count rate in the fission chambers and the fission rate in the centre of the core is given by

$$N_1 = a_1 \cdot \hat{R}_{25} + b_1 \hat{R}_{28} \tag{A1}$$

$$N_2 = a_2 \cdot \hat{R}_{25} + b_2 \hat{R}_{28} \tag{A2}$$

where

$N_1$; $N_2$ : counts/sec in the two fission chambers

$a_i$; $b_i$ : (i = 1, 2) known constants typical for the detectors

$\hat{R}_{25}$; $\hat{R}_{28}$ : fission rate in the core centre for $^{235}U$ and $^{238}U$, respectively

The relation between the count rate in the gas-scintillator and the fission chambers is described by

$$N = c_1 \cdot N_1 = c_2 N_2 \tag{A3}$$

where

$N$ : counts/sec in $^3$He-scintillator

$c_1$; $c_2$ : constants to be determined in the calibration

The desired expression for the scintillator efficiency is given by

$$\epsilon = \frac{\text{number of counts/sec in the scintillator}}{\text{total number of fissions/sec in the core}} =$$

$$= \frac{N}{\int_V m_{25} \cdot R_{25}(r,z)dV + \int_V m_{28} \cdot R_{28}(r,z)dV} \tag{A4}$$

where

$V$ : volume of the core

$R_{25}(r,z)$ : the fission rate for $^{235}U$ at point r, z in the core

$R_{28}(r,z)$ : " " " " $^{238}U$ " " " " " "

$m_{25}$ : number of $^{235}U$-atoms/volume unit

$m_{28}$ : " " $^{238}U$- " " "

$m_{25}$ and $m_{28}$ are constant within the core.

Now we define

$$k_{25} = \frac{\int_V R_{28}(r,z)dV}{\hat{R}_{25} \cdot V}$$

$$k_{28} = \frac{\int_V R_{28}(r,z)dV}{\hat{R}_{28} \cdot V}$$

which with Eq (A4) yields

$$\epsilon = \frac{N}{m_{25} \cdot V \cdot \hat{R}_{25} \cdot k_{25} + m_{28} \cdot V \cdot \hat{R}_{28} \cdot k_{28}} \qquad (A5)$$

When $k_{25}$ and $k_{28}$ have been determined Eqs (A1), (A2), (A3) together with (A5) will give the value of $\epsilon$.

# APPENDIX 3

## Experimental results

| Exp run | Core | $\tau$ ms | $\frac{\overline{m^2}-\overline{m}^2}{\overline{m}}$ | $\epsilon \cdot 10^4$ | $D_\nu$ | $-\rho^{(1)} \cdot 10^5$ | The expression within the brackets in Eq (9) |
|---|---|---|---|---|---|---|---|
| 1 | 3 | 5 | 6.08 ± 0.13 (1.3)[1] | 4.07 ± 0.09 (1.1) | 0.804 ± 0.015 (0.9) | 56.6 ± 3.0 (0.4) | 0.991 |
| 2 | 3 | 5 | 4.79 ± 0.11 (1.4) | 3.05 ± 0.07 (1.1) | 0.804 ± 0.015 (0.9) | 56.6 ± 3.0 (0.4) | 0.992 |
| 3 | 3 | 9 | 5.61 ± 0.12 (1.3) | 4.12 ± 0.09 (1.1) | 0.804 ± 0.015 (0.9) | 94.5 ± 3.0 (0.4) | 0.995 |
| 4 | 3 | 9 | 4.45 ± 0.09 (1.4) | 3.03 ± 0.07 (1.1) | 0.804 ± 0.015 (0.9) | 94.5 ± 3.0 (0.4) | 0.995 |
| 5 | 5 | 9 | 5.19 ± 0.10 (1.2) | 3.29 ± 0.07 (1.1) | 0.815 ± 0.021 (1.3) | 26.3 ± 3.0 (0.4) | 0.995 |
| 6 | 5 | 3 | 5.30 ± 0.13 (1.5) | 3.21 ± 0.07 (1.2) | 0.815 ± 0.021 (1.3) | 26.3 ± 3.0 (0.4) | 0.984 |
| 7 | 8 | 5 | 5.10 ± 0.10 (1.2) | 3.25 ± 0.07 (1.1) | 0.806 ± 0.015 (0.9) | 38.5 ± 3.0 (0.4) | 0.990 |
| 8 | 8 | 7 | 4.59 ± 0.09 (1.3) | 2.89 ± 0.06 (1.1) | 0.806 ± 0.015 (0.9) | 38.5 ± 3.0 (0.4) | 0.993 |

| Exp run | d μs | A(d) | B(d) | $\frac{\tau-d}{\tau}$ | Correction due[2] to delayed neutrons | $\beta_{eff} \cdot 10^3$ | Error (%) | |
|---|---|---|---|---|---|---|---|---|
| | | | | | | | Type I | Type II |
| 1 | 1.5 | 0.006 | 0.964 ± 0.014 (0.8) | 1.000 | 0.995 | 7.22 | 1.3 | 1.7 |
| 2 | 3.4 | 0.010 | 0.939 ± 0.028 (1.5) | 0.999 | 0.995 | 7.13 | 1.4 | 2.1 |
| 3 | 1.5 | 0.003 | 0.968 ± 0.015 (0.8) | 1.000 | 1.000 | 7.29 | 1.3 | 1.7 |
| 4 | 3.4 | 0.005 | 0.941 ± 0.028 (1.5) | 1.000 | 1.000 | 7.10 | 1.4 | 2.1 |
| 5 | 3.4 | 0.012 | 0.949 ± 0.024 (1.3) | 1.000 | 0.984 | 7.49 | 1.2 | 2.2 |
| 6 | 3.4 | 0.012 | 0.948 ± 0.024 (1.3) | 0.999 | 0.995 | 7.21 | 1.5 | 2.2 |
| 7 | 3.4 | 0.012 | 0.947 ± 0.024 (1.3) | 0.999 | 0.993 | 7.30 | 1.2 | 2.0 |
| 8 | 3.4 | 0.011 | 0.951 ± 0.024 (1.3) | 1.000 | 0.991 | 7.40 | 1.3 | 2.0 |

[1] The numbers in parentheses are the percentage errors in the final value of $\beta_{eff}$ from each parameter

[2] This correction originates from the third term in Eq (3) and is applied to $\left[\frac{\overline{m^2}-\overline{m}^2}{\overline{m}} - 1\right]$

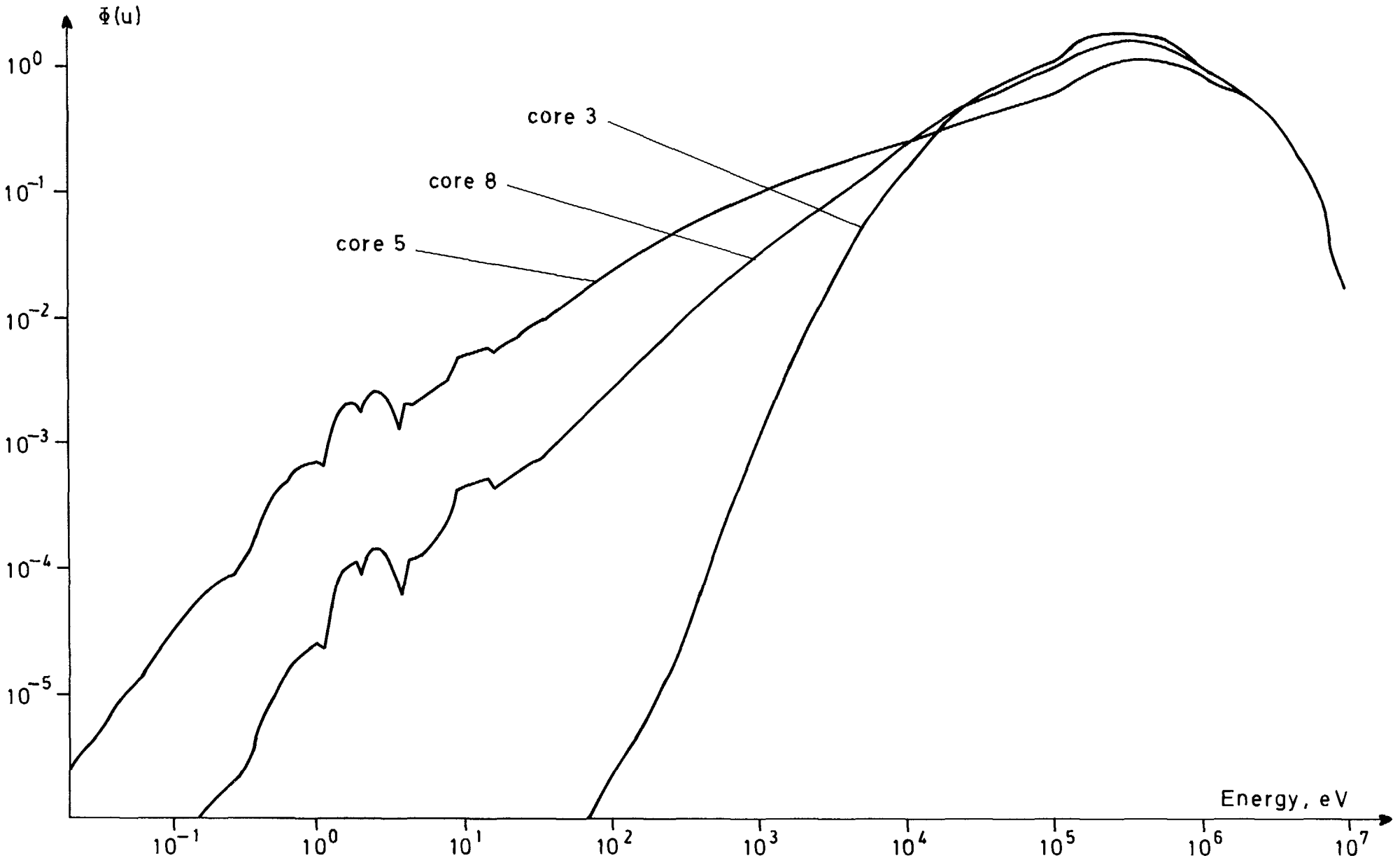


Fig. 1 Calculated central neutron spectra for FRO cores 3, 5 and 8.

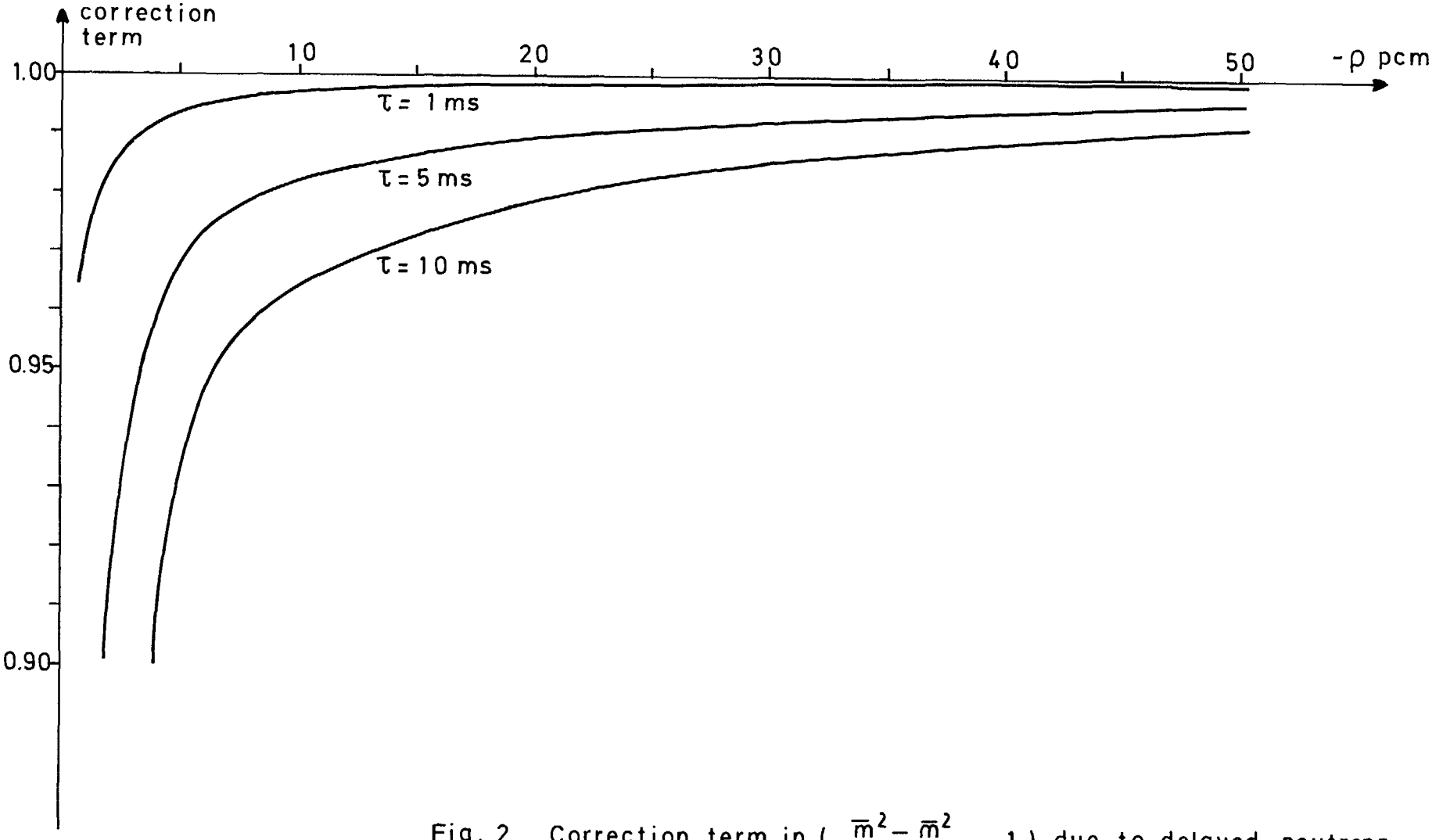


Fig. 2. Correction term in $\left( \frac{\bar{m}^2 - \bar{m}^2}{\bar{m}} - 1 \right)$ due to delayed neutrons.

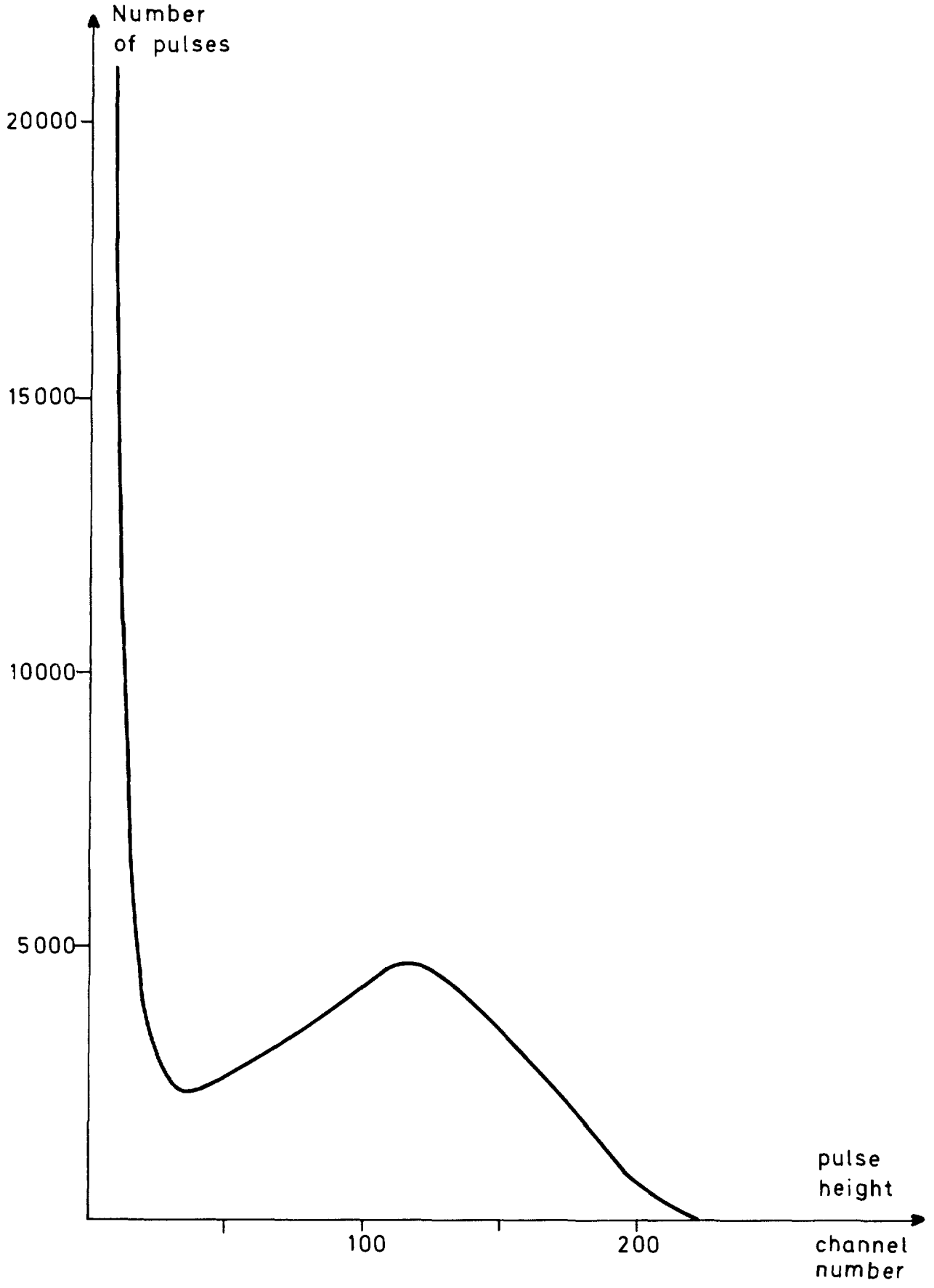


Fig. 3 Pulse height distribution from a $^{242}$Cm-Be-source.

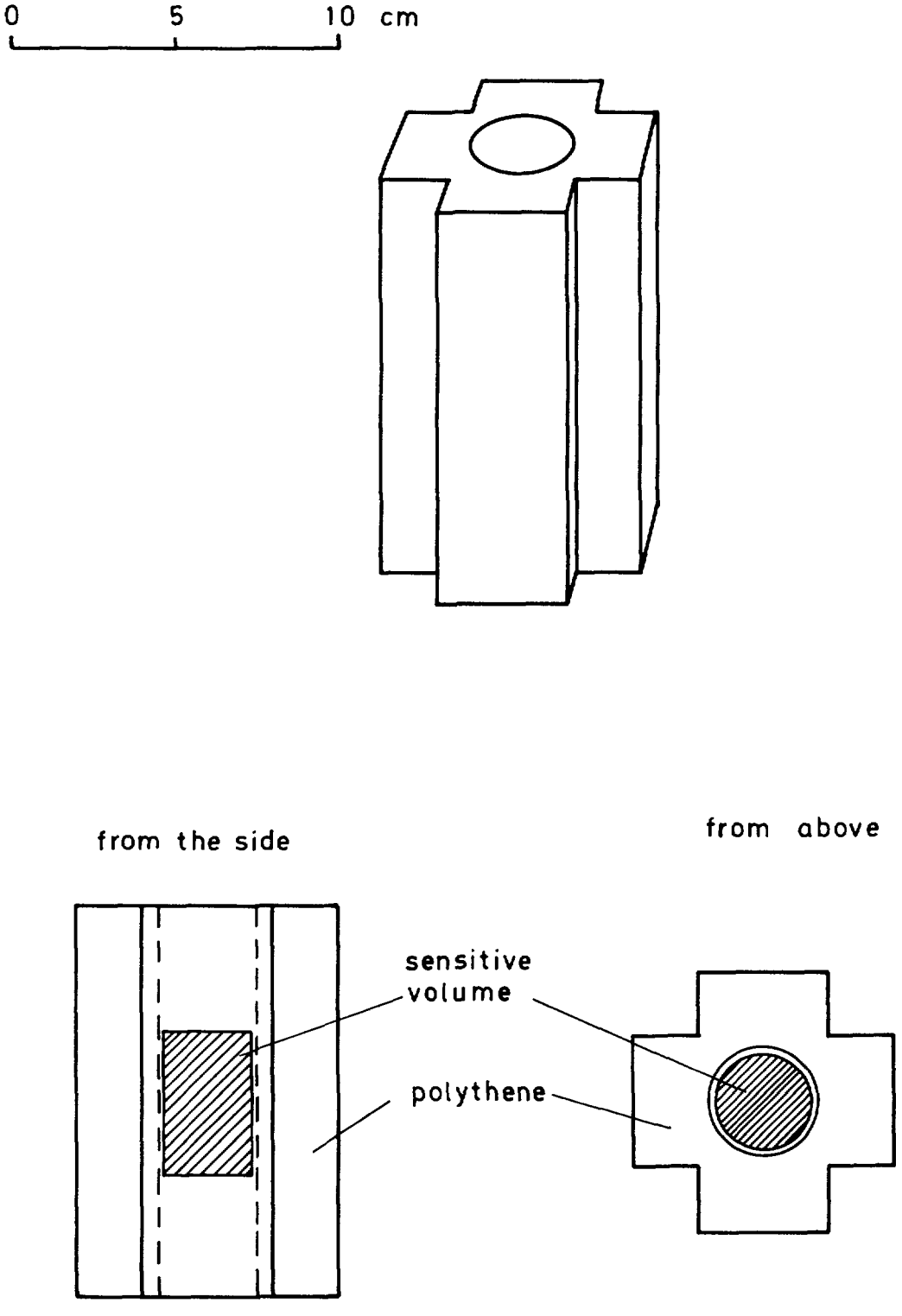


Fig. 4 The detector with surrounding polythene

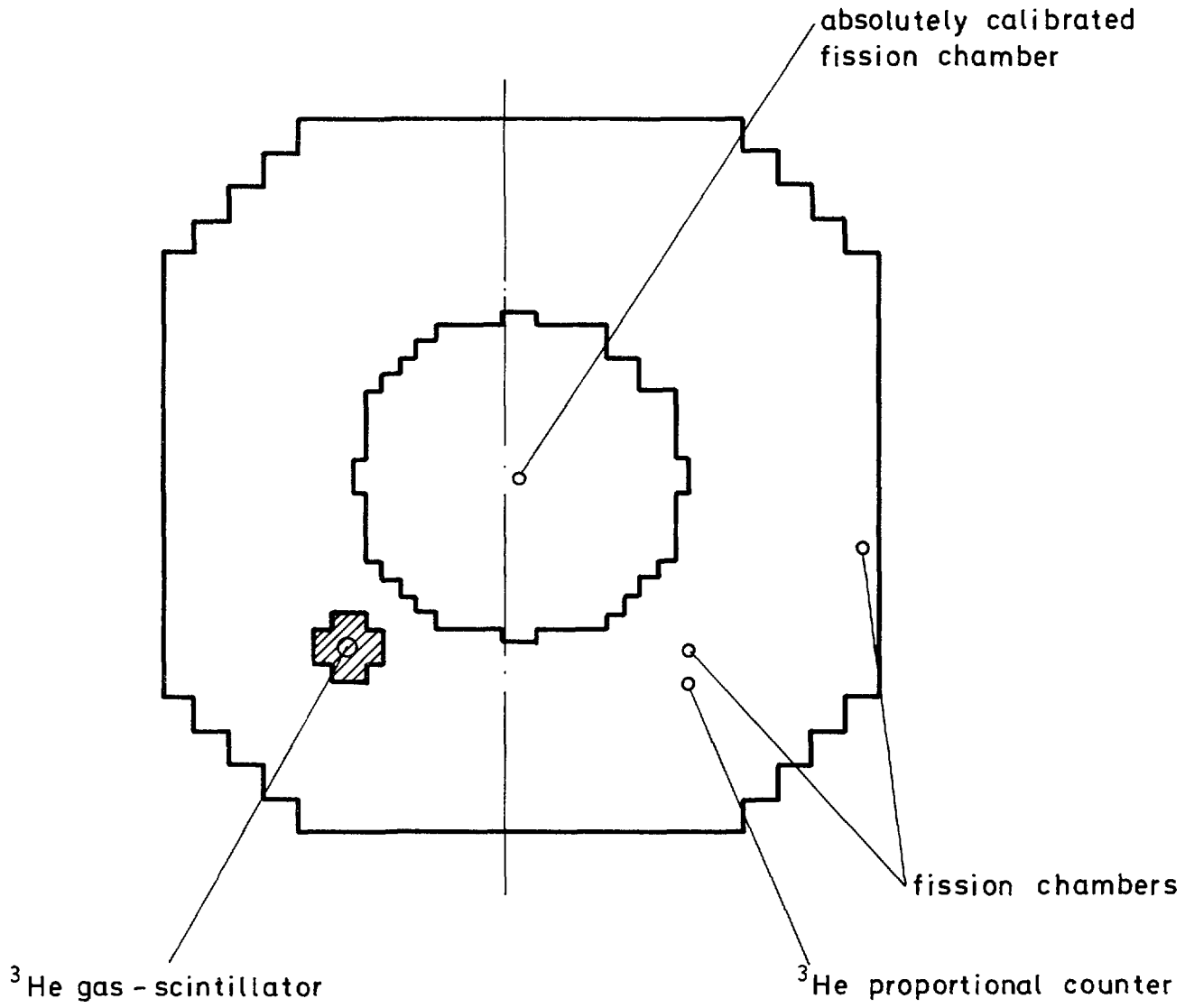


Fig 5. The detectors placed in the reactor.

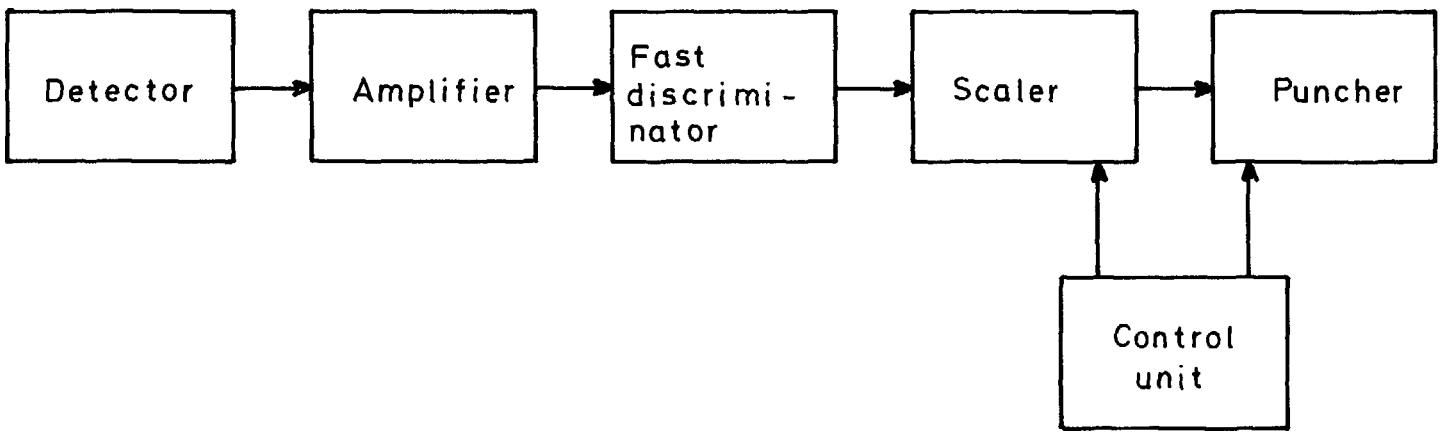


Fig. 6 Block diagram of the electronics

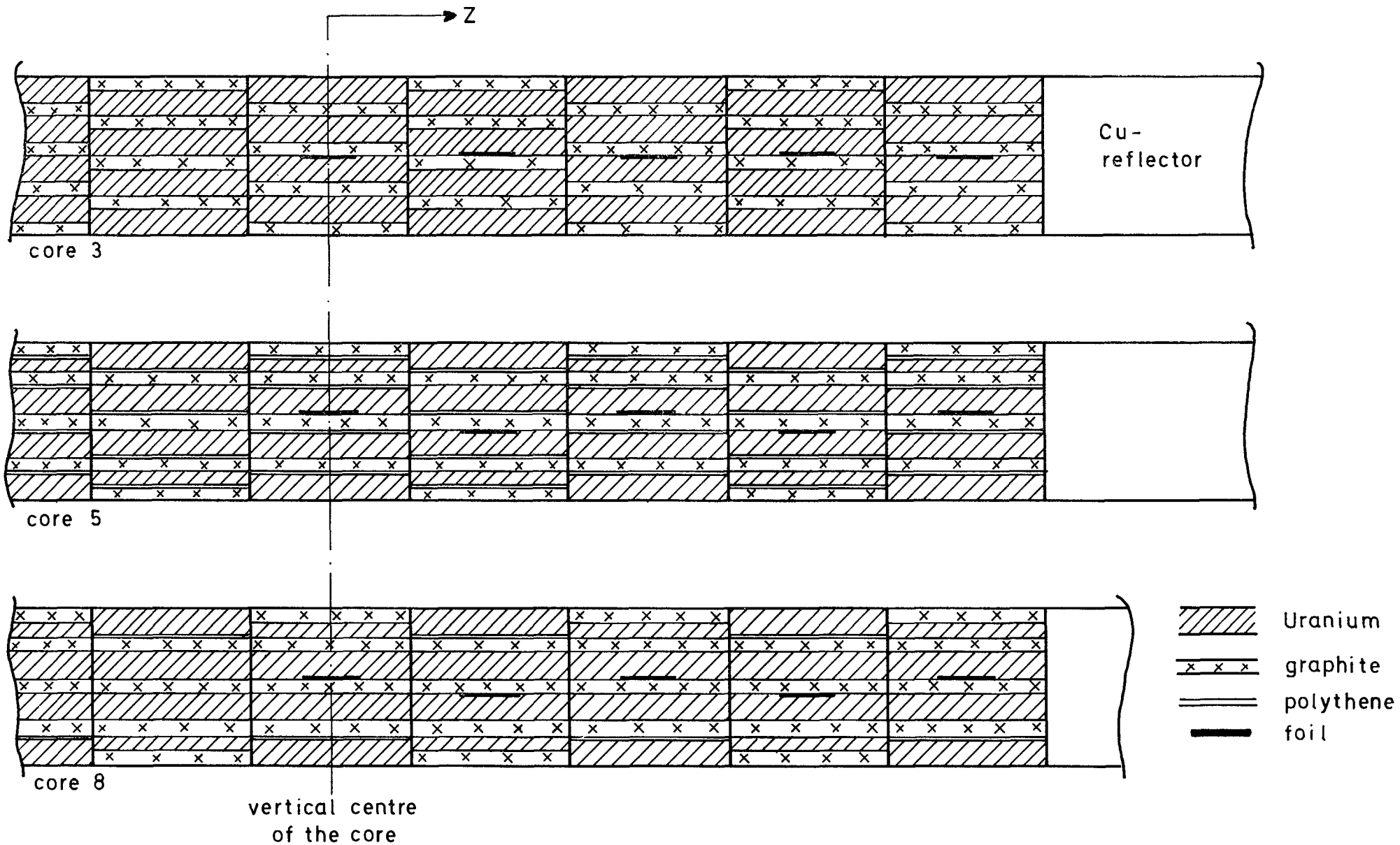


Fig. 7 Position of the foils in the fuel elements.

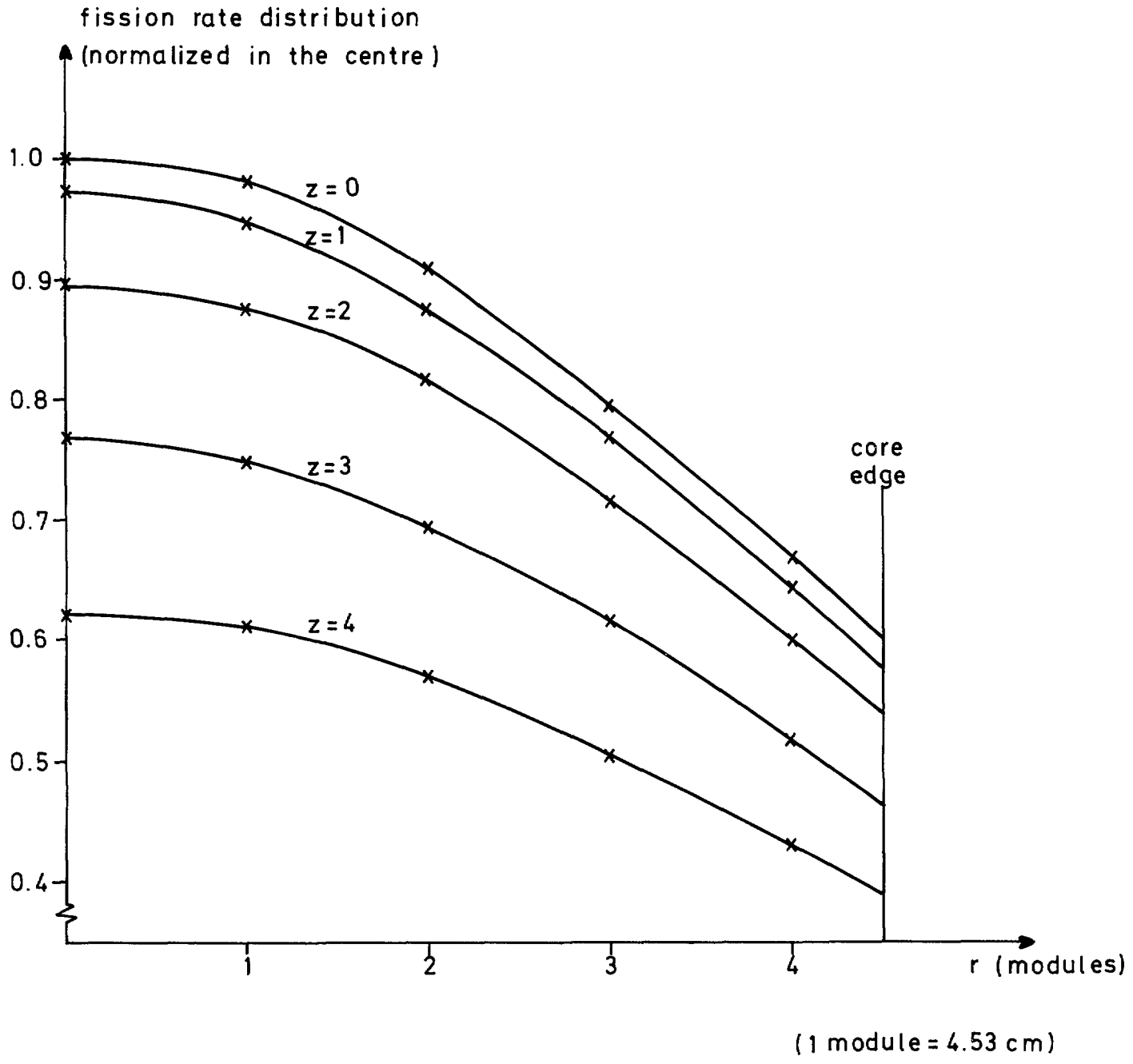


Fig. 8 Space distribution of the $^{235}U$ fission rate in core 3.

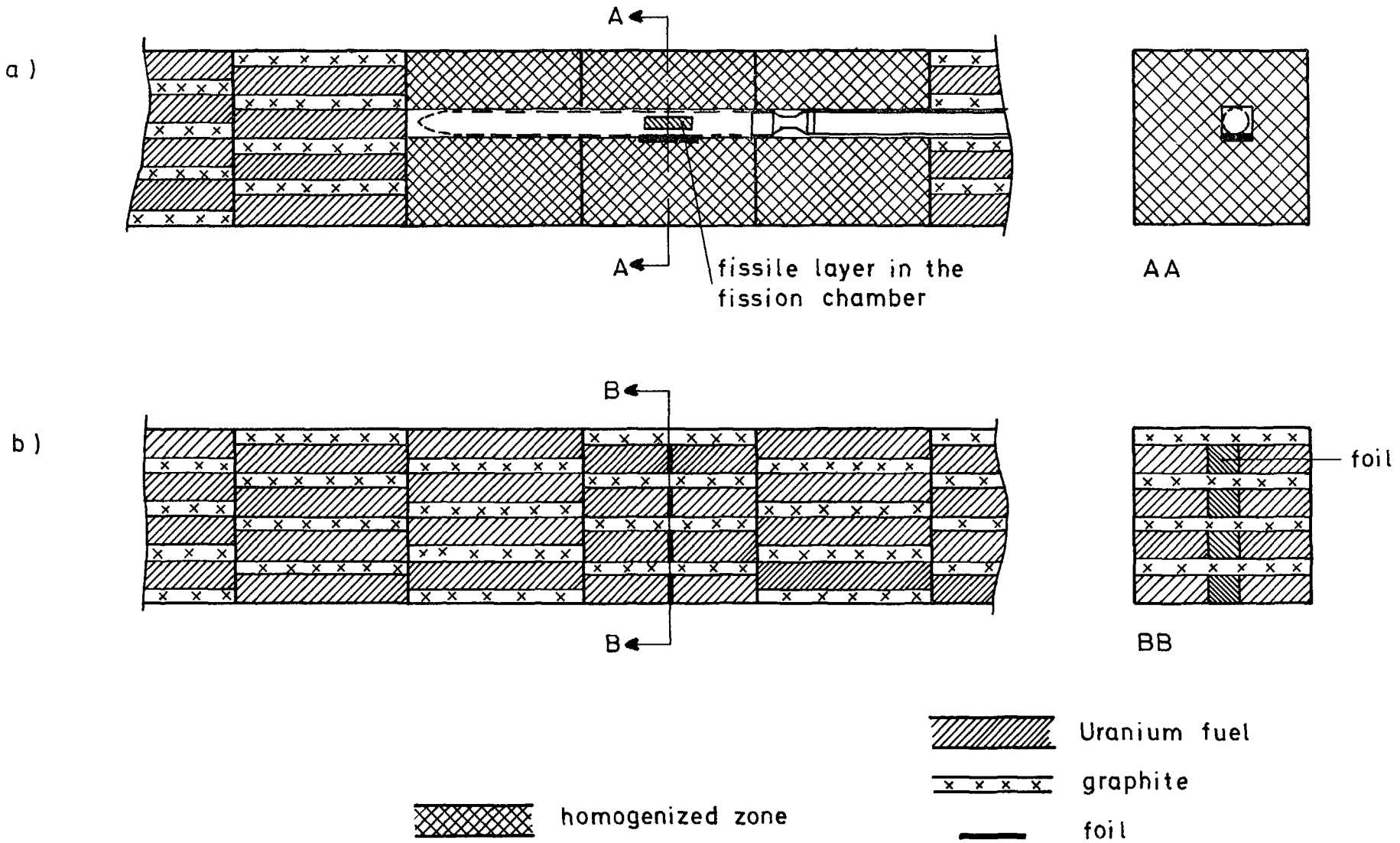


Fig. 9 The central fuel element in core 3 with a) a foil placed near the fission chamber

b) the foils placed in the "heterogenous"way

## LIST OF PUBLISHED AE-REPORTS

1–370 (See back cover earlier reports.)

381. The 93.54 keV lever $^{91}$Sr, and evidence for 3-neutron states above N=50. By S. G. Malmskog and J. McDonald 1970. 24 p. Sw. cr. 10:–.
382. The low energy level structure of $^{191}$Ir. By S. G. Malmskog, V. Berg, A. Bäcklin and G Hedin. 1970. 24 p Sw cr 10:–.
383. The drinking rate of fish in the Skagerack and the Baltic. By J. E. Larsson. 1970. 16 p. Sw. cr. 10:–.
384. Lattice dynamics of Nacl, KCl, RbCl and RbF. By G. Raunio and S. Rolandson. 1970. 26 p. Sw. cr. 10:–.
385. A neutron elastic scattering study of chromium, iron and nickel in the energy region 1.77 to 2.76 MeV. By B. Holmqvist, S. G. Johansson, G. Lodin, M Salama and T. Wiedling. 1970. 26 p. Sw. cr. 10:–.
386. The decay of bound isobaric analogue states in $^{28}$Si and $^{32}$Si using (d. n$\gamma$) reactions. By L. Nilsson, A Nilsson and I. Bergqvist. 1970. 34 p. Sw. cr. 10–.
387. Transition probabilities in $^{189}$Os. By S. G. Malmskog, V. Berg and A. Bäcklin. 1970. 40 p. Sw. cr. 10:–.
388. Cross sections for high-energy gamma transition from MeV neutron capture in $^{206}$Pb. By I. Bergqvist, B. Lundberg and L. Nilsson. 1970. 16 p. Sw. cr. 10:–.
389. High-speed, automatic radiochemical separations for activation analysis in the biological and medical research laboratory. By K. Samsahl. 1970. 18 p. Sw. cr. 10:–.
390. Use of fission product Ru-106 gamma activity as a method for estimating the relative number of fission events in U-235 and Pu-239 in low-enriched fuel elements. By R. S. Forsyth and W. H. Blackadder. 1970. 26 p. Sw. cr. 10:–.
391. Half-life measurements in $^{134}$I. By V. Berg and A. Höglund. 1970. 16 p. Sw. cr. 10:–.
392. Measurement of the neutron spectra in FRO cores 5, 9 and PuB-5 using resonance sandwich detectors. By T. L. Andersson and M. N. Qazi. 1970. 30 p. Sw. cr. 10:–.
393. A gamma scanner using a Ge(Li) semi-conductor detector with the possibility of operation in anti-coincidence mode. By R. S. Forsyth and W. H. Blackadder. 1970. 22 p. Sw. cr. 10:–.
394. A study of the 190 keV transition in $^{141}$La. By B. Berg, A. Höglund and B. Fogelberg. 1970 22 p. Sw cr. 10:–.
395. Magnetoacoustic waves and instabilities in a Hall-effect-dominiated plasma. By S. Palmgren. 1970. 20 p. Sw. cr. 10:–.
396. A new boron analysis method. By J. Weitman, N. Dåverhög and S. Farvolden. 1970. 26 p. Sw. cr. 10:–.
397. Progress report 1969. Nuclear chemistry. 1970. 39 p. Sw. cr. 10:–.
398. Prompt gamma radiation from fragments in the thermal fission of $^{235}$U. By H. Albinsson and L. Lindow. 1970. 48 p. Sw. cr. 10:–.
399. Analysis of pulsed source experiments performed in copper-reflected fast assemblies. By J. Kockum. 1970. 32 p. Sw. cr. 10:–.
400. Table of half-lives for excited nuclear levels. By S. G. Malmskog. 1970. 33 p. Sw. cr. 10:–.
401. Needle type solid state detectors for in vivo measurement of tracer activity. By A. Lauber, M. Wolgast. 1970. 43 p. Sw. cr. 10:–.
402. Application of pseudo-random signals to the Agesta nuclear power station By P-Å. Bliselius. 1970. 30 p. Sw. cr. 10:–.
403. Studies of redox equilibria at elevated temperatures 2. An automatic divided-function autoclave and cell with flowing liquid junction for electrochemical measurements on aqueous systems. By. K. Johnsson, D. Lewis and M. de Pourbaix. 1970. 38 p. Sw. cr. 10:–.
404. Reduction of noise in closed loop servo systems. By K. Nygaard. 1970. 23 p. Sw. cr. 10:–.
405. Spectral parameters in water-moderated lattices. A survey of experimental data with the aid of two-group formulae. By E. K. Sokolowski. 1970. 22 p. Sw. cr. 10:–.
406. The decay of optically thick helium plasmas, taking into account ionizing collisions between metastable atoms or molecules. By J. Stevefelt. 1970. 18 p. Sw. cr. 10:–.
407. Zooplankton from Lake Magelungen, Central Sweden 1960-63. By E. Almquist. 1970. 62 p. Sw. cr. 10:–.
408. A method for calculating the washout of elemental iodine by water sprays. By E. Bachofner and R. Hesböl. 1970. 24 p. Sw. cr. 10:–.
409. X-ray powder diffraction with Guinier–Hägg focusing cameras. By A. Brown. 1970. 102 p. Sw. cr. 10:–.
410. General physic section Progress report. Fiscal year 1969/70. By J. Braun. 1970. 92 p. Sw. cr. 10:–.
411. In-pile determination of the thermal conductivity of $UO_2$ in the range 500–2 500 degrees centigrade. By J-A Gyllander. 1971. 70 p. Sw. cr. 10:–.
412. A study of the ring test for determination of transverse ductility of fuel element canning. By G. Anevi and G. Östberg. 1971. 17 p. Sw. cr. 15:–.
413. Pulse radiolysis of Aqueous Solutions of aniline and substituted anilines. By H. C. Christensen. 1971. 40 p. Sw. cr. 15:–.
414. Radiolysis of aqueous toluene solutions. By H. C. Christensen and R. Gustafson. 1971. 20 p. Sw. cr. 15:–.
415. The influence of powder characteristics on process and product parameters in $UO_2$ pelletization. By U. Runfors. 1971. 32 p. Sw. cr. 15:–.
416. Quantitative assay of Pu239 and Pu240 by neutron transmission measurements. By E. Johansson. 1971. 26 p. Sw. cr 15:–.
417. Yield of prompt gamma radiation in slow-neutron induced fission of $^{235}$U as a function of the total fragment kinetic energy. By H. Albinsson. 1971. 38 p. Sw. cr. 15:–.
418. Measurements of the spectral light emission from decaying high pressure helium plasmas. By J. Stevefelt and J. Johansson. 1971. 48 p. Sw. cr. 15:–.
419. Progress report 1970. Nuclear chemistry. 1971. 32 p. Sw. cr. 15:–.
420. Energies and yields of prompt gamma rays from fragments in slow-neutron induced fission of $^{235}$U. By H. Albinsson. 1971. 56 p. Sw. cr. 15:–.
421. Decay curves and half-lives of gamma-emitting states from a study of prompt fission gamma radiation. By H. Albinsson. 1971. 28 p. Sw. cr. 15:–.
422. Adjustment of neutron cross section data by a least square fit of calculated quantities to experimental results. Part 1. Theory. By H. Häggblom. 1971. 28 p. Sw. cr. 15:–.
423. Personnel dosimetry at AB Atomenergi during 1969. By J. Carlsson and T. Wahlberg. 1971. 10 p. Sw. cr. 15:–.
424. Some elements of equilibrium diagrams for systems of iron with water above 100°C and with simple chloride, carbonate and sulfate melts. By D. Lewis. 1971. 40 p. Sw. cr. 15:–.
425. A study of material buckling in uranium-loaded assemblies of the fast reactor FR0. By R. Håkansson and L. I. Tirén. 1971. 32 p. Sw. cr. 15:–.
426. Dislocation line tensions in the noble metals, the alkali metals and $\beta$-Brass. By B. Pettersson and K. Malén. 1971. 14 p. Sw. cr. 15:–.
427. Studies of fine structure in the flux distribution due to the heterogeneity in some FR0 cores. By T. L. Andersson and H. Häggblom. 1971. 32 p. Sw. cr. 15:–
428. Integral measurement of fission-product reactivity worths in some fast reactor spectra. By T. L. Andersson. 1971. 36 p. Sw. cr. 15:–.
429. Neutron energy spectra from neutron induced fission of $^{235}$U at 0.95 MeV and of $^{238}$U at 1.35 and 2.02 MeV. By E. Almén, B. Holmqvist and T. Wiedling. 1971. 16 p. Sw. cr. 15:–.
430. Optical model analyses of experimental fast neutron elastic scattering data. By B. Holmqvist and T. Wiedling. 1971. 238 p. Sw. cr. 20:–.
431. Theoretical studies of aqueous systems above 25°C. 1. Fundamental concepts for equilibrium diagrams and some general features of the water system. By Derek Lewis. 1971. 27 p. Sw. cr. 15:–.
432. Theoretical studies of aqueous systems above 25°C . 2. The iron – water system. By Derek Lewis. 1971. 41 p. Sw. cr. 15:–.
433. A detector for (n,$\gamma$) cross section measurements. By J Hellström and S. Beshai. 1971. 22 p. Sw. cr. 15:–.
434. Influence of elastic anisotropy on extended dislocation nodes. By B. Pettersson. 1971. 27 p. Sw cr. 15:–.
435. Lattice dynamics of CsBr. By S. Rolandson and G. Raunio. 1971. 24 p. Sw. cr. 15:–.
436. The hydrolysis of iron (III) and iron (II) ions between 25°C and 375°C. By Derek Lewis. 1971.16 p. Sw. cr. 15:–.
437. Studies of the tendency of intergranular corrosion cracking of austenitic Fe-Cr-Ni alloys in high purity water at 300°C. By W. Hübner, B. Johansson and M. de Pourbaix. 1971. 30 p. Sw. cr. 15:–.
438. Studies concerning water-surface deposits in recovery boilers. By O. Strandberg, J. Arvesen and L. Dahl. 1971. 132 p. Sw. cr. 15:–.
439. Adjustment of neutron cross section data by a least square fit of calculated quantities to experimental results. Part II. Numerical results. By H. Häggblom. 1971. 70 p. Sw. cr. 15:–.
440. Self-powered neutron and gamma detectors for in-core measurements. By O. Strindehag. 1971. 16 p. Sw. cr. 15:–.
441. Neutron capture gamma ray cross sections for Ta, Ag, In and Au between 30 and 175 keV. By J. Hellström and S. Beshai. 1971. 30 p. Sw. cr. 15:–.
442. Thermodynamical properties of the solidified rare gases. By I. Ebbsjö. 1971. 46 p. Sw. cr. 15:–.
443. Fast neutron radiative capture cross sections for some important standards from 30 keV to 1.5 MeV. By J. Hellström. 1971. 22 p. Sw. cr. 15:–.
444. A Ge (Li) bore hole probe for in situ gamma ray spectrometry. By A. Lauber and O. Landström. 1971. 26 p. Sw. cr. 15:–.
445. Neutron inelastic scattering study of liquid argon. By K. Sköld, J. M. Rowe, G. Ostrowski and P. D. Randolph. 1972. 62 p. Sw. cr. 15:–.
446. Personnel dosimetry at Studsvik during 1970. By L. Hedlin and C.-O. Widell. 1972.. 8 p. Sw. cr. 15:–.
447. On the action of a rotating magnetic field on a conducting liquid. By E. Dahlberg. 1972. 60 p. Sw. cr. 15:–.
448. Low grade heat from thermal electricity production. Quantity, worth and possible utilisation in Sweden. By J. Christensen. 1972. 102 p. Sw. cr. 15:–.
449. Personnel dosimetry at studsvik during 1971. By L. Hedlin and C.-O. Widell. 1972. 8 p. Sw. cr. 15:–.
450. Deposition of aerosol particles in electrically charged membrane filters. By L. Ström. 1972. 60 p. Sw. cr. 15:–.
451. Depth distribution studies of carbon in steel surfaces by means of charged particle activation analysis with an account of heat and diffusion effects in the sample. By D. Brune, J. Lorenzen and E. Witalis. 1972. 46 p. Sw. cr. 15:–.
452. Fast neutron elastic scattering experiments. By M. Salama. 1972. 98 p. Sw. cr. 15:–.
453. Progress report 1971. Nuclear chemistry. 1972. 21 p. Sw. cr. 15:–.
454. Measurement of bone mineral content using radiation sources. An annotated bibliography. By P. Schmeling. 1972. 64 p. Sw. cr. 15:–.
455. Long-term test of self-powered deectors in HBWR. By M. Brakas, O. Strindehag and B. Söderlund. 24 p. 1972. Sw. cr. 15:–.
456. Measurement of the effective delayed neutron fraction in three different FR0-cores. By L. Moberg and J. Kockum. 1972. Sw. cr. 15:–.

### List of published AES-reports (In Swedish)

1. Analysis by means of gamma spectrometry. By D. Brune. 1961. 10 p. Sw. cr. 6:–.
2. Irradiation changes and neutron atmosphere in reactor pressure vessels-some points of view. By M. Grounes. 1962. 33 p. Sw. cr. 6:–.
3. Study of the elongation limit in mild steel. By G. Östberg and R. Attermo. 1963. 17 p. Sw. cr. 6:–.
4. Technical purchasing in the reactor field. By Erik Jonson. 1963. 64 p. Sw. cr. 8:–.
5. Agesta nuclear power station. Summary of technical data, descriptions, etc. for the reactor. By B. Lilliehöök. 1964. 336 p. Sw. cr. 15:–.
6. Atom Day 1965. Summary of lectures and discussions. By S. Sandström. 1966. 321 p. Sw. cr. 15:–.
7. Building materials containing radium considered from the radiation protection point of view. By Stig O. W. Bergström and Tor Wahlberg. 1967. 26 p. Sw. cr. 10:–.
8. Uranium market. 1971. 30 p. Sw. cr. 15:–.
9. Radiography day at Studsvik. Tuesday 27 april 1971. Arranged by AB Atomenergi, IVA's Committee for nondestructive testing and TRC AB. 1971. 102 p. Sw. cr. 15:–.
10. The supply of enriched uranium. By M. Mårtensson. 1972. 53 p. Sw. cr. 15:–.

Additional copies available from the Library of AB Atomenergi, Fack, S-611 01 Nyköping 1, Sweden.

EOS-tryckerierna, Stockholm 1972